Check for updates

ARTICLE   OPEN

Preclinical dose response study shows *NR2E3* can attenuate retinal degeneration in the retinitis pigmentosa mouse model *Rho*$^{P23H+/-}$

Shannon M. McNamee[1,5], Natalie P. Chan[1,5], Monica Akula [1], Marielle O. Avola[1], Maiya Whalen[1], Kaden Nystuen[2], Pushpendra Singh[3], Arun K. Upadhyay[3], Margaret M. DeAngelis[4] and Neena B. Haider [1 ✉]

© The Author(s) 2024

Retinitis pigmentosa (RP) is a heterogeneous disease and the main cause of vision loss within the group of inherited retinal diseases (IRDs). IRDs are a group of rare disorders caused by mutations in one or more of over 280 genes which ultimately result in blindness. Modifier genes play a key role in modulating disease phenotypes, and mutations in them can affect disease outcomes, rate of progression, and severity. Our previous studies have demonstrated that the nuclear hormone receptor 2 family e, member 3 (*Nr2e3*) gene reduced disease progression and loss of photoreceptor cell layers in *Rho*$^{P23H-/-}$ mice. This follow up, pharmacology study evaluates a longitudinal *NR2E3* dose response in the clinically relevant heterozygous *Rho*^{P23H} mouse. Reduced retinal degeneration and improved retinal morphology was observed 6 months following treatment evaluating three different *NR2E3* doses. Histological and immunohistochemical analysis revealed regions of photoreceptor rescue in the treated retinas of *Rho*$^{P23H+/-}$ mice. Functional assessment by electroretinogram (ERG) showed attenuated photoreceptor degeneration with all doses. This study demonstrates the effectiveness of different doses of *NR2E3* at reducing retinal degeneration and informs dose selection for clinical trials of *Rho*^{P23H}-associated RP.

Gene Therapy; https://doi.org/10.1038/s41434-024-00440-6

INTRODUCTION

Retinitis pigmentosa (RP) is the most common form of inherited blindness. RP is a heterogeneous disease that varies in age of onset, rate of progression and genetic etiology based on the mutation and gene impacted [1–5]. Retinitis pigmentosa affects 1 in 4000 individuals worldwide [6, 7]. RP diseases include syndromic and non-syndromic forms with over 200 unique genetic mutations associated with disease onset [8–14]. There is currently only one type of treatment approved to treat a specific form of RP, voretigene neparvovec (Luxturna®) is approved for treatment in patients with biallelic *RPE65* gene mutations [15–18]. Additionally, over 40% of RP cases cannot be genetically diagnosed [19]. While there is great heterogeneity in RP disease, the common shared pathology is degeneration of photoreceptor (PR) cells. The genes and mechanisms causing photoreceptor degeneration can vary and the cumulative degenerative outcome is influenced by a mutational load on the system that includes the primary mutation and modifier genes among other factors [20]. Our previous publication revealed the novel finding that the modifier gene *Nr2e3* can treat retinal degeneration in several mouse models of RP [19].

Modifier genes are defined as allelic variants within a normal population, and can significantly impact the onset, progression, and severity of diseases [21–24]. Studies of multiple diseases including spinal muscular atrophy, spinocerebellar ataxia type 1, dystonia, epileptic encephalopathy, cystic fibrosis, and retinal degeneration show the effect of modifier genes and their impact on disease phenotypes altered by shifted genetic backgrounds [25–33]. Mutations in the modifier gene nuclear hormone receptor *NR2E3* are associated with several types of retinal degeneration including clumped pigmentary retinal degeneration (CPRD), Goldmann–Favre syndrome (GFS), enhanced S-cone syndrome (ESCS), and autosomal dominant retinitis pigmentosa (adRP) [34]. The variable phenotypes of *NR2E3*-associated retinal degeneration suggest modifier genes could be influencing disease manifestation and outcomes. *Nr2e3* plays a major role in the retina by regulating the development and maintenance of photoreceptor cells, and regulating gene networks in pathways including ER stress, neuroprotection, photoreceptor function, apoptosis, immune response, and cell survival, and thereby impacting homeostasis of the retina [19, 35–41]. Modifier genes such as *NR2E3* could thus be a more effective therapeutic agent and especially beneficial in RP cases where the primary mutation cannot be identified. Previous publications by our lab examined the effectiveness of *Nr2e3* as a therapeutic for *NR2E3*-associated RP as well as other forms of RP that do not possess an *NR2E3* mutation [19].

Although RP is a rare disease, mutations in the Rhodopsin gene represent about 40% of all adRP cases [42]. Additionally, there are

[1]Schepens Eye Research Institute, Massachusetts Eye and Ear, Department of Ophthalmology, Harvard Medical School, Boston, MA, USA. [2]University of Massachusetts Amherst, Amherst, MA, USA. [3]Ocugen, Inc, Malvern, PA, USA. [4]Department of Ophthalmology, Jacobs School of Medicine & Biomedical Sciences, University at Buffalo, Buffalo, NY, USA. [5]These authors contributed equally: Shannon M. McNamee, Natalie P. Chan. ✉email: neena_haider@hms.harvard.edu

more than 150 known mutations in Rhodopsin and the Rho^{P23H} mutation accounts for about 10% of Rho related adRP in the United States alone [42–45]. The Rho^{P23H} mutation creates a misfolded protein that is not processed properly and accumulates in the endoplasmic reticulum (ER) [19, 45]. The accumulation of these aberrant Rho proteins causes cellular stress [43, 46–48]. Patients with this mutation usually experience night-blindness followed by a progressive loss of their visual field [42–48]. This was a pharmacological study to demonstrate the efficacy of dosage and longitudinal impact of $NR2E3$ modifier gene therapy to treat retinal degeneration in the $Rho^{P23H+/-}$ mouse when administered during early/intermediate degeneration. Treated animals were assessed 1, 3, and 6 months after dose administration to track the degree of longitudinal rescue of degeneration. The Rho^{P23H} mouse is a model for human Retinitis Pigmentosa 4 (RP-4). These mice harbor a substitution of the amino acid proline with histidine at position 23 resulting in protein misfolding and degradation from an aberrant message [19, 45]. Heterozygous Rho^{P23H} mice were used for this study, as they are more clinically relevant with adRP features including gradual loss of rods and scotopic ERG function followed by loss of cones and photopic ERG function [45, 49, 50]. $Rho^{P23H+/-}$ mice exhibit rapid photoreceptor degeneration from postnatal day (P) 15 to P30 that progresses to gradual degeneration over time [45, 49, 50]. The outer nuclear layer (ONL) thickness of a P30 $Rho^{P23H+/-}$ retina is about 30–40% less than a normal wild-type retina and continues to gradually decrease with age [45, 49]. $Rho^{P23H+/-}$ mice retain a majority of their photoreceptors; however, the cells in the inner and outer segments show structural disorganization and as mice age the outer segments (OS) become shorter [44]. P35 mice possess shorter rod OS and by P63, have about half the normal amount of rod nuclei compared to wild-type mice [45]. Scotopic ERG responses are severely reduced by P41 and are nearly undetectable by P170 [45]. In comparison, homozygous mice exhibit severe rapid retinal degeneration by P23 with almost complete loss of photoreceptors by P63 [45]. It is important to note, our previous study of $Nr2e3$ therapeutic utilized $Rho^{P23H-/-}$ mice which possess an abnormal fundus phenotype whereas this study utilized $Rho^{P23H+/-}$ mice that have a normal fundus phenotype [19]. This study demonstrates that low, mid, and high doses of AAV5-$hNR2E3$ can slow retinal degeneration in the $Rho^{P23H+/-}$ mouse for at least 6 months following treatment when administered during early/intermediate disease.

MATERIALS AND METHODS
Animal maintenance
This study was performed in accordance with the Association for Research in Vision and Ophthalmology (ARVO) Statement for the Use of Animals in Ophthalmic and Vision Research and the Guide for the Care and Use of Laboratory Animals of the National Institute of Health. The Schepens Eye Research Institute vivarium housed and bred animals under standard conditions, 68-74 °F and 12-h light/dark cycle, for the course of this study. All animals and procedures used in this study were approved by the Schepens Eye Research Institute Animal Care and Use Committee (Protocol Number: 2020N000178) in accordance with the Animal Welfare Act Regulations. B6.129S6(Cg)-Rhotm1.1Kpal/J ($Rho^{P23H-/-}$; Jax stock #017628) [45] and C57BL6/J (B6, Jax stock #000664) mice were obtained from Jackson Laboratories, Bar Harbor, ME. $Rho^{P23H+/-}$ animals were generated by crossing $Rho^{P23H-/-}$ knock-in males with B6 females [51].

Scientific rigor and reproducibility
Estimation of the required sample size for each analysis and quantification was conducted via a power calculation using G*Power 3.1 software analysis. 90% power and 30% difference with a significance level of 0.05 was provided by a minimum of eight animals per experimental group according to means and standard deviations defined in previous publications. All procedures performed in this study used a standardized

protocol for consistent replication. Bias was avoided using a randomized and double blinded study method with several trained individuals. A minimum of 8 biological replicates were performed per dose and timepoint for statistical significance. Exclusion criteria included animals with unresolved surgical trauma, premature unintended death, or cataracts. Approximately 10% of the 100 animals used in this study were excluded from the results. No gender bias was observed between males (~48.04%) and females (~51.96%) used in this study.

Statistical analysis
Mean ± standard error of the mean (SEM) represents technical variations in rescue in electroretinography and outer nuclear layer thickness due to focal delivery of $NR2E3$. Statistical significance was analyzed in graphs using either two-way analysis of variance (ANOVA) or t test. Cell count analysis was performed to analyze the difference between untreated and each dose treated retinas 6 months after treatment. The mean peak scotopic A- and B-wave amplitudes of untreated and treated animals for each dose and timepoint were compared.

Genotyping
The quick lysis sodium hydroxide method was used for DNA isolation of tail biopsies from the $Rho^{P23H+/-}$ mice. Samples were amplified with the transgene specific primers P23H-F: GGTAGCACTGTTGGGCATCT and P23H-R: GACCCCACAGAGACAAGCTC [52]. Approximately 50 ng of DNA was used for polymerase chain reaction (PCR) amplification in a reaction volume of 10 µL. Reactions consisted of 10 µM each of forward and reverse primer, 40 mM of dNTP mix, 10x buffer with $MgCL_2$, and 5 U/ml AmpliTaq DNA polymerase. Reaction parameters were 94 °C for 2 min followed by 39 cycles at 94 °C for 15 s, 60 °C for 30 s, and 72 °C for 1 min ending with 72 °C for 5 min. 2% ethidium bromide-stained agarose gels were used to separate amplicons and visualize bands under UV light. Wild-type amplicon is 150 base pairs (bp), and the mutant amplicon is 320 bp. The large difference in amplicon size is due to the amplification of the knock-in transgene in mutant mice [52]. Heterozygous animals were genotyped using the protocol recommended by Jackson Laboratory, Bar Harbor, ME.

AAV5-$hNR2E3$ dose preparation
Three doses were evaluated. The low dose was chosen to be one log unit lower than the therapeutic (mid) dose to examine the lower limit of dose effectiveness, while the high dose was chosen to be 4 times greater than the mid to evaluate potential dose toxicity. The human $NR2E3$ gene was packaged into AAV5 capsid with optimized regulatory elements to create the drug product (AAV5-$hNR2E3$). Ocugen, INC. supplied the GLP vector drug product and formulation buffer (10 mM sodium phosphate, 180 mM sodium chloride, and 0.001% Poloxamer 188 (PF-68) at pH 7.3 ± 0.5). The drug product was diluted with formulation buffer to achieve the following concentrations: 2×10^{11} Vg/ml, 2×10^{12} Vg/ml, 8×10^{12} Vg/ml. The intended low (1×10^8 vgc/eye), mid (1×10^9 vgc/eye), and high (4×10^9 vgc/eye) doses used for subretinal injection were aliquoted from these dilutions.

Subretinal injection
All AAV5-$hNR2E3$ doses were delivered via subretinal injection into the right eye of $Rho^{P23H+/-}$ mice. P30 mice were anesthetized with ketamine/xylazine by intraperitoneal (IP) injection using a 0.5" 25G needle. An incision was made in the sclera with a 25G needle and a total volume of 0.5 µL of either low, mid, or high dose AAV5-$hNR2E3$ was manually administered into the subretinal space [19]. The contralateral (left) eye of treated animals was used as the untreated control in this study. The untreated eye received either no injection, a mock injection with no vector, or a mock injection with saline buffer to demonstrate that the injection itself does not impact the results.

Clinical examination
Fundus imaging of the clinical phenotype was performed using a Micron IV Retinal Imaging Camera and Stream Pix software (Phoenix Research Laboratories, Pleasanton, CA, USA) on treated and untreated $Rho^{P23H+/-}$ mice. After administering anesthesia via IP injection of ketamine/xylazine with a 25G needle, 1 drop of 1% Tropicamide was applied to dilate pupils and Genteal was applied to moisturize the eye. Mice were then placed on a platform and aligned using a real-time fundus image of the retina to center the optic nerve before capturing [15].
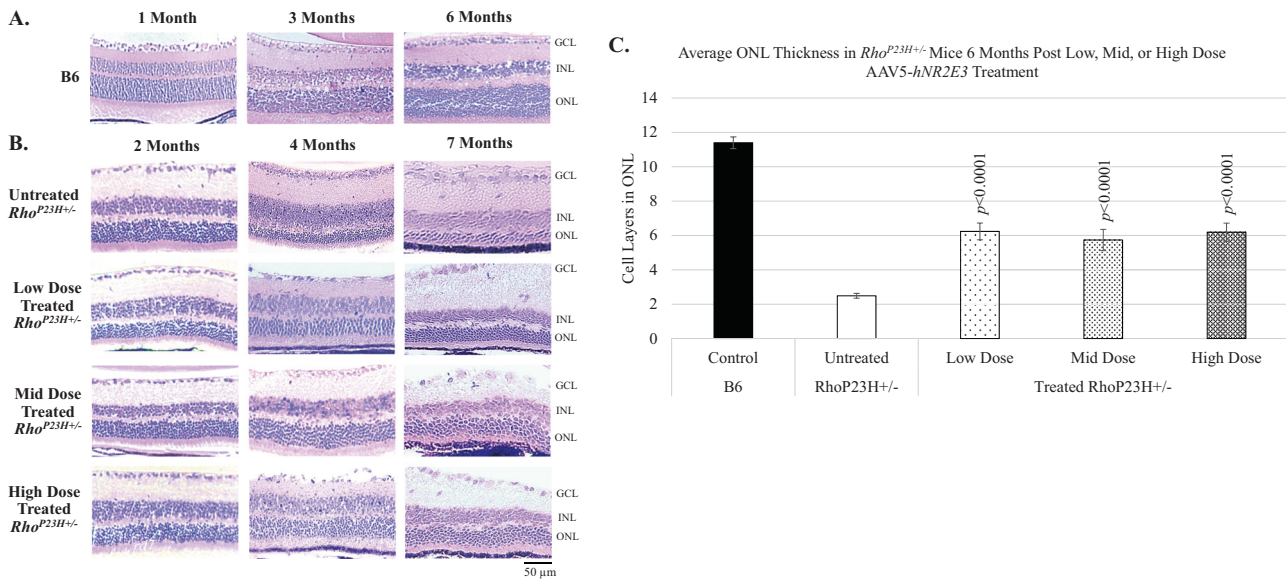
Fig. 1 Treatment with AAV5-*hNR2E3* slows ONL degeneration in *Rho^P23H+/−* retinas for all doses. ONL thickness in untreated *Rho^P23H+/−* animals compared to the thickness of rescued regions in AAV5-*hNR2E3* treated *Rho^P23H+/−* mice. **A** C57BL/6J (B6) normal histology of 1-, 3-, and 6-month retinas. **B** Comparison of untreated and *NR2E3* treated *Rho^P23H+/−* animals injected at 1 month of age and collected at 1-, 3-, and 6-months post-injection (animal ages 2, 4, and 7 months). **C** Wild type and untreated *Rho^P23H+/−* retinas (7 months old) counted in comparison to 6-months post-treatment (animal ages 7 months) counts of 1-month *NR2E3* treated *Rho^P23H+/−* retinas. $p < 0.0001$ for all 3 doses compared with untreated *Rho^P23H+/−* eyes. Serial sections of central retina counted over 100 μm. Results are mean ± SEM. Low Dose 1×10^8 vg/eye, Mid Dose 1×10^9 vg/eye, High Dose 4×10^9 vg/eye. GCL: Ganglion Cell Layer; INL: Inner Nuclear Layer; ONL: Outer Nuclear Layer. Scale bar = 50 μm. $N \geq 4$.

Electroretinography
Electroretinography (ERG) analysis was performed on AAV5-*hNR2E3* treated and untreated mouse eyes with the Espion Visual Electrophysiology System (Diagnosys LLC, Lowell, MA, USA). Mice were dark-adapted overnight in a dark chamber and anesthetized with ketamine/xylazine by IP injection using a 0.5" 25G needle. Pupils were dilated with a drop of 1% Tropicamide and kept moist using a topical application of Genteal. Mice were positioned on to the platform and the ground electrode was placed at the base of the tail followed by the reference electrode placed just underneath the skin of the scalp. Two gold loop electrodes (Diagnosys LLC) were aligned and placed flush on the eyes of the mouse. Dark- and light-adapted ERGs were performed and recorded using the previously described protocol [19]. Peak scotopic A- and B-wave amplitudes were taken from each animal and averaged for each dose and timepoint compared to the untreated and wild-type amplitudes.

Histology
Hematoxylin and eosin (H/E) staining of retinal layers was performed using a standard protocol established in the lab [19]. Following euthanasia, eyes were immediately cauterized to mark dorsal/ventral orientation and to allow penetration of fixative. Eyes were fixed in 4% paraformaldehyde (PFA) in 1x PBS overnight at 4 °C and paraffin embedded. 5 μm serial sections were cut across 100 μm of retinal depth. Sections were deparaffinated in xylene and ethanol dips. Then, sections were stained with Harris hematoxylin and eosin Y. Coverslips were mounted with Permount and images were taken using a Leica DMI6000 microscope (Leica Microsystems, Wetzlar, Germany). A minimum of 3 personnel counted photoreceptor cell layers in the outer nuclear layer (ONL) in a double blinded method [19, 53]. Photoreceptor rescue was quantified by comparing the number of cell layers in the ONL of *NR2E3* treated and untreated *Rho^P23H+/−* retinas and B6 control retinas.

Immunohistochemistry
Immunohistochemical (IHC) analysis was performed on 5 μm paraffin embedded sections using standardized lab protocols [19]. Sections were deparaffinated in a series of xylene and ethanol dips followed by a rinse in PBS. Antigen sites were unmasked by soaking the sections in sodium citrate buffer. Sections were blocked with 2% normal horse serum (S-2000 Vector Labs, CA) in 1× PBS at room temperature for an hour. The primary antibodies rhodopsin (mouse monoclonal, Millipore MAB5356), blue opsin

(rabbit polyclonal, Millipore AB5407), and green/red opsin (rabbit polyclonal, Millipore AB5405) were applied at 1:200 dilutions in PBS and incubated at 4 °C overnight. The following day sections were rinsed with PBS and the corresponding secondary antibody was applied in the dark in a 1:400 dilution in PBS: Alexa Fluor 488 goat anti-mouse (Invitrogen A11001) for rhodopsin and Alexa Fluor 488 goat anti-rabbit (Invitrogen A11008) for green and blue opsin slides. These slides were then incubated for an hour in the dark and finally nuclei were labeled with 4,6-Diamidino-2-Phenylindole, Dihydrochloride (DAPI, dilactate, Invitrogen D3571). Opsin labeling was visualized and imaged using a Leica DMI6000 fluorescent microscope (Leica Microsystems, Wetzlar, Germany) [19].

RESULTS
AAV5-*hNR2E3* delivery in three different doses in *Rho^P23H+/−* animals rescues photoreceptor degeneration for at least 6 months
NR2E3 was administered in a low, mid, or high dose by subretinal delivery during early/intermediate disease progression and photoreceptor rescue was evaluated 1-, 3-, and 6-months post-treatment in *Rho^P23H+/−* mice. The retina of a normal mouse is composed of the ONL (10–12 layers of rod and cone photo-receptor nuclei), inner nuclear layer (INL, 5–6 layers of inner retinal cells), and a single ganglion cell layer (GCL) [19]. *Rho^P23H+/−* mice lose 30–40% of ONL thickness by P30 followed by gradual decreases until about 6 months of age [45, 49]. Histological analysis of *Rho^P23H+/−* animals dosed with AAV5-*hNR2E3* at P30 showed improved photoreceptor survival up to 6 months after treatment. H/E staining showed improved ONL thickness in treated retinas compared to untreated retinas for the 3- and 6-months post timepoints (Fig. 1B). The ONL thickness was sustained across the disease progression from 2 months (1-month post-treatment) to 7 months (6-months post-treatment) of age. Results indicate that all three *NR2E3* doses can reduce degeneration and sustain photoreceptor survival in *Rho^P23H+/−* mice for at least 6 months after treatment. Counts of the photoreceptor nuclei layers in the ONL of *Rho^P23H+/−* animals treated at P30 and collected 6 months later showed that photoreceptor survival was
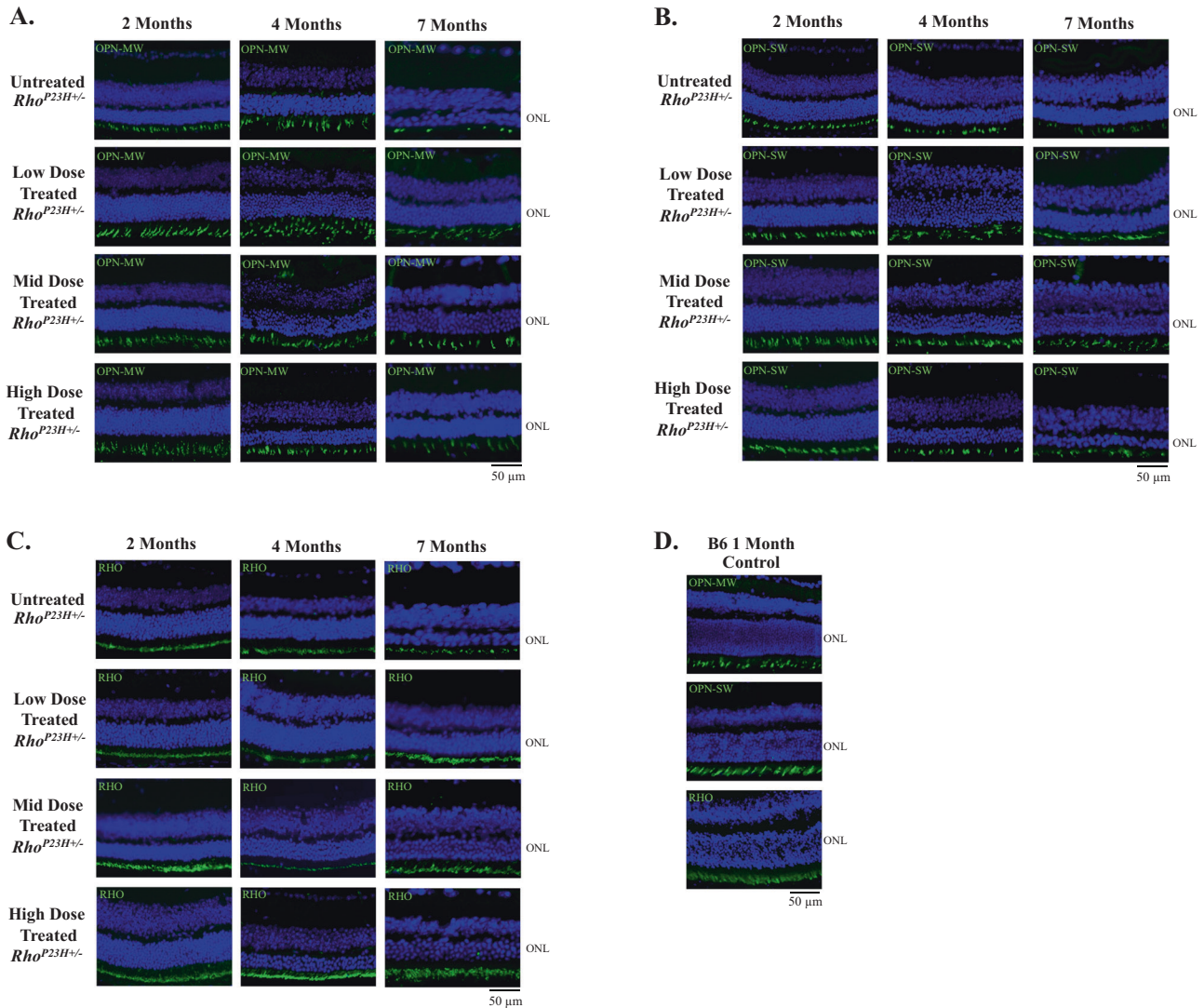
A.

B.

C.

D.

Fig. 2 Treatment with low, mid, or high dose AAV5-*hNR2E3* maintained opsin expression in *Rho*$^{P23H+/-}$ animals. Expression comparison between untreated and *NR2E3* treated *Rho*$^{P23H+/-}$ animals injected at 1 month of age and evaluated 1-, 3-, and 6-months post-injection labeled with **A** green opsin (OPN-MW), **B** blue opsin (OPN-SW), and **C** rhodopsin (RHO) antibodies. **D** C57BL/6J (B6) normal expression of green opsin (OPN-MW), blue opsin (OPN-SW), and rhodopsin (RHO). Green opsin (OPN-MW) and blue opsin (OPN-SW) labeling showed maintained expression in treated animals. Rhodopsin (RHO) labeling showed restored expression in treated animals. Dapi is indicated in blue and opsins are shown in green. Low Dose 1×10^8 vg/eye, Mid Dose 1×10^9 vg/eye, High Dose 4×10^9 vg/eye. Scale bar = 50 μm. $N = 8$.

significantly increased compared to untreated animals (Fig. 1C; $p < 0.0001$). All three doses showed rescue with a p-value less than 0.0001. The ONL thickness did not return to the normal range indicating that degeneration is likely not being reversed but that treatment with *NR2E3* during early/intermediate disease can slow or halt degeneration.

NR2E3 dose therapy preserved cone and rod opsin expression in *Rho*$^{P23H+/-}$ animals up to 6 months after treatment during early/intermediate disease progression

Immunohistochemical analysis examined the longitudinal efficacy of a low, mid, and high dose of AAV5-*hNR2E3* to rescue cone opsin and rhodopsin expression in *Rho*$^{P23H+/-}$ mice. In the *Rho*$^{P23H+/-}$ mouse, about half of rod photoreceptor nuclei are lost by 2 months of age followed by slow progressive loss of cones until around 6 months of age [45]. *Rho*$^{P23H+/-}$ animals were dosed at P30 with *NR2E3*, and eyes were collected at 1-, 3-, and 6- months post-treatment. Treated animals showed preserved expression of all opsins compared to untreated animals for all doses lasting up to 6 months after treatment (Fig. 2). Most notable was the

preservation of rhodopsin expression in *NR2E3* treated eyes compared to untreated. This can be attributed to the age of *NR2E3* administration. Since almost half of all rods are lost by 2 months of age, administration of the therapeutic at P30 can rescue a majority of the rod photoreceptors from degeneration. Expression of all opsins was observed in all timepoints and doses for treated *Rho*$^{P23H+/-}$ mice compared to untreated but was not restored to normal levels 6 months later.

Three different doses of AAV5-*hNR2E3* preserved photoreceptor function in *Rho*$^{P23H+/-}$ animals treated during early/intermediate disease

Dark-adapted ERG analysis was performed to examine the efficacy of low, mid, and high doses of AAV5-*hNR2E3* at rescuing rod- and cone-photoreceptor driven responses. Disease progression in the *Rho*$^{P23H+/-}$ mouse model results in the progressive loss of photoreceptor function with severely diminished scotopic ERG responses by around 6 months of age [45]. Through our previous studies, we were able to show improved ERG responses in *Rho*$^{P23H-/-}$ mice treated with *Nr2e3* [19]. A- and B-wave peak
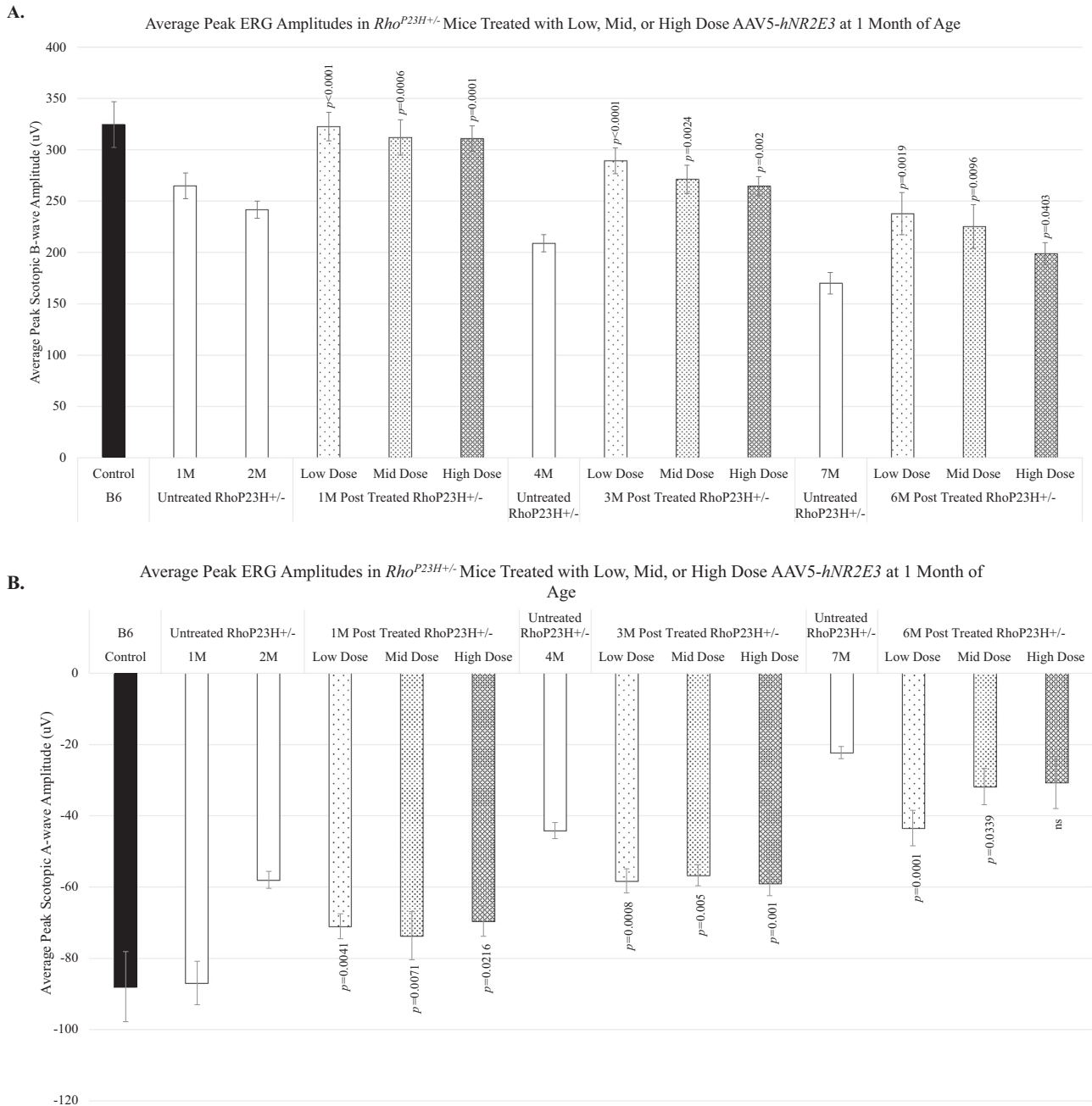
A.

Average Peak ERG Amplitudes in $Rho^{P23H+/-}$ Mice Treated with Low, Mid, or High Dose AAV5-hNR2E3 at 1 Month of Age

Average Peak Scotopic B-wave Amplitude (uV)

Control B6 | 1M Untreated RhoP23H+/- | 2M | Low Dose | Mid Dose | High Dose | 4M Untreated RhoP23H+/- | Low Dose | Mid Dose | High Dose | 7M Untreated RhoP23H+/- | Low Dose | Mid Dose | High Dose

1M Post Treated RhoP23H+/- ; 3M Post Treated RhoP23H+/- ; 6M Post Treated RhoP23H+/-

p<0.0001, p=0.0006, p=0.0001, p<0.0001, p=0.0024, p=0.002, p=0.0019, p=0.0096, p=0.0403

B.

Average Peak ERG Amplitudes in $Rho^{P23H+/-}$ Mice Treated with Low, Mid, or High Dose AAV5-hNR2E3 at 1 Month of Age

Average Peak Scotopic A-wave Amplitude (uV)

B6 Control 1M | Untreated RhoP23H+/- 2M | 1M Post Treated RhoP23H+/- Low Dose Mid Dose High Dose | Untreated RhoP23H+/- 4M | 3M Post Treated RhoP23H+/- Low Dose Mid Dose High Dose | Untreated RhoP23H+/- 7M | 6M Post Treated RhoP23H+/- Low Dose Mid Dose High Dose

p=0.0041, p=0.0071, p=0.0216, p=0.0008, p=0.005, p=0.001, p=0.0001, p=0.0339, ns

Fig. 3   AAV5-hNR2E3 treated $Rho^{P23H+/-}$ mice showed preserved retinal function for all doses. $Rho^{P23H+/-}$ mice were treated with low, mid, or high dose NR2E3 at 1 month of age and assessed 1-, 3-, and 6-months post-treatment (2, 4, and 7 months of age) with ERG. **A** There was a significant increase in peak scotopic B-wave amplitude of treated vs untreated animals at 1 month ($p < 0.0006$–0.0001), 3 months ($p < 0.002$–0.0001) and 6 months ($p < 0.05$–0.002) post-treatment. **B** Scotopic A-wave peak amplitudes were significantly higher in treated $Rho^{P23H+/-}$ mice compared to untreated 1 month ($p \leq 0.0216$–0.0041), 3 months ($p \leq 0.005$–0.0008), and 6 months ($p \leq 0.0339$–0.0001) post-treatment. Low Dose 1×10^8 vg/eye; Mid Dose 1×10^9 vg/eye, High Dose 4×10^9 vg/eye. Results are mean ± SEM. $N \geq 5$.

amplitudes were analyzed to evaluate photoreceptor functionality for perceiving light and transmitting the signal. The A-wave response measures the ability of photoreceptors to receive light and transform that information into an electrical signal. B-wave responses measure the ability of photoreceptors to send the electrical signal to second-order neurons [54]. $Rho^{P23H+/-}$ animals treated at P30 maintained normal levels of scotopic peak B-wave amplitudes in treated retinas compared to untreated retinas lasting over 6 months after treatment (Fig. 3A; $p < 0.0403$–0.0001). The most robust amplitudes were apparent 1-month post-treatment for all doses with the low (Fig. 3A; $p < 0.0001$) and high

(Fig. 3A; $p = 0.0001$) doses having the most significant preservation of B-wave at that time. The low dose continued showing the most significant B-wave preservation of the three doses at the 3- and 6-month post-treatment timepoints. Noteworthy, ERG responses decreased over time for all doses of NR2E3 treatment but remained significant and within normal levels for at least 6 months after treatment compared to untreated $Rho^{P23H+/-}$. This suggests a significant attenuation of degeneration as the treated values still remain above or within the values of the 2-month untreated responses with the exception of the 6-months post high dose. Similar to the B-wave trends, the 1-month post timepoint

showed the most robust preservation of peak scotopic A-wave amplitudes and the low dose showed the most significant preservation of amplitudes at all timepoints (Fig. 3B; $p \leq 0.0041–0.0001$). Similarly to the B-waves, the A-wave amplitude preservation decreased over time for all doses supporting the notion that degeneration is slowed significantly by *NR2E3* treatment.

DISCUSSION

Diseases such as RP present a major obstacle to the medical community. The large phenotypic variations in RP stemming from factors like environment, epigenetics, gene mutations, and allelic heterogeneity make finding effective treatments difficult [55]. However, there is great promise in modifier genes as therapeutics for various forms of RP. The modifier gene *Nr2e3*, which has a key role in several homeostasis pathways such as phototransduction, cell survival, ER stress, oxidative stress, apoptosis, immunity, metabolism, and neuroprotection, has been used in previous studies to reduce disease progression and even rescue retinal degeneration [19, 56]. Our previous publication revealed that *Nr2e3* gene therapy can rescue degeneration in several models of RP including the more severe $Rho^{P23H-/-}$ mouse. Adeno-associated virus serotype 5 (AAV5) was the chosen viral vector for this study based on our previous publication that tested gene delivery with AAV2.7m8, AAV5 and AAV8 as well as its safety and efficiency at transducing retinal pigment epithelium (RPE) and photoreceptor cells [19, 57–63]. This was a pharmacological study to inform the longitudinal effectiveness of several doses of AAV5-hNR2E3 in $Rho^{P23H+/-}$ mice for treating Rho^{P23H}-associated RP. The novel components of this study were the examination of a low, mid, and high dose of AAV5-hNR2E3, examination of dose effectiveness up to 6 months after administration, and the use of the heterozygous Rho^{P23H} mouse model instead of the more severe homozygous model from our previous study. The heterozygous model is more representative of both the genotype and phenotype of human Rho^{P23H}-associated RP. Analysis showed significant improvement of photoreceptor survival and function in $Rho^{P23H+/-}$ mice for all three doses lasting at least 6 months after administration of *NR2E3* therapeutic. Preserved expression of blue opsin, green opsin, and rhodopsin proteins was also observed in all doses for up to 6 months. Note that H/E and immunohisto-chemistry revealed regions of rescue in the treated retinas due to the focal delivery of *NR2E3* into the subretinal space. Based on this evidence, histological, molecular, and functional analysis showed that *NR2E3* overexpression can slow degeneration and improve the disease outcome over time in the $Rho^{P23H+/-}$ mouse. Clinical examination of the fundus of treated vs. untreated $Rho^{P23H+/-}$ mice 1-, 3-, and 6-months post-treatment revealed no adverse effects on the retina as a result of *NR2E3* therapy (Supplemental Fig. 1). Additionally, no abnormal systemic responses or overt toxic effects were observed in daily behavior or gross pathology following therapy administration. Comparison of untreated control $Rho^{P23H+/-}$ fundus and H/E data demonstrated no obvious impacts of the injection itself on the retina in eyes that received either a mock injection, mock and saline buffer injection, or no injection (Supplemental Fig. 2).

$Rho^{P23H+/-}$ mice are functional nulls in which the protein does not undergo complete glycosylation, becomes trapped, and degrades within the endoplasmic reticulum (ER) and/or Golgi apparatus [19, 45]. *Nr2e3* has been shown in recent studies to play a role in the ER stress pathway. More specifically it is believed to target inositol-requiring enzyme 1 (*Ire1*), a cell survival and ER stress factor, which was found in our previous publication to be upregulated following *Nr2e3* administration in various models of RP including $Rho^{P23H-/-}$ [19]. ER stress activates *Ire1* which encodes for an ER-resident transmembrane protein and is a key regulator of the most highly conserved branch of the unfolded protein response (UPR) signaling pathway [64–66]. *Ire1* activation helps to clear misfolded proteins from the ER including misfolded Rho^{P23H} by upregulating several ER chaperones that partially ameliorate the misfolding defect in Rho^{P23H} proteins [46–48, 66]. Therefore, upregulation of *Ire1* via *NR2E3* administration may prevent the degradation of Rho^{P23H} protein and promote escape from the ER into the retinal outer segments thus delaying degeneration from ER stress.

Unlike our prior study on *Nr2e3* treatment in $Rho^{P23H-/-}$ mice at P0 (prior to disease onset) and P21 (early/intermediate disease progression), this study examined administration of *NR2E3* therapy at P30, which falls in early/intermediate disease, in heterozygous Rho^{P23H} mice. Treatment prior to disease onset or as early into disease progression as possible is obviously the optimal treatment time for the majority of therapeutics and diseases as the amount of damage done by disease is minimal. However, this is often not feasible in the clinical setting as diseases are not usually diagnosed until symptoms arise, which can be in the early to intermediate stages of disease when significant damage has already occurred in systems. The results of this study demonstrate that *NR2E3*, while more robust when administered prior to onset, can reduce degeneration in the early/intermediate stages of disease and for at least 6 months after treatment. It is also important to note that *NR2E3* maintained ERG responses in $Rho^{P23H+/-}$ animals at normal levels for at least 6 months compared to untreated.

Selecting the optimal dosage for treatment of degeneration is also imperative for the clinical setting. Based on our results, no single dose of *NR2E3* was better across the board or caused any gross abnormalities, although the low dose had more robust rescue of ERG responses for all timepoints. Thus, the low dose of *NR2E3* therapy is the optimal choice for treatment in $Rho^{P23H+/-}$ as it will slow degeneration for at least 6 months and likely prompt the lowest immune response.

Overall, the results of this study demonstrate the ability of various doses of AAV5-hNR2E3 administered during early/intermediate progression to slow retinal degeneration in the $Rho^{P23H+/-}$ mouse for a minimum of 6 months. Overexpression of *NR2E3* can restore homeostasis in the $Rho^{P23H+/-}$ mouse by resetting key *Nr2e3*-associated pathways including the ER stress pathway therefore reducing degeneration and improving photoreceptor function and survival. The results of this study strongly support the potential of *NR2E3* as a gene modifier therapy capable of treating retinal degeneration in non-*NR2E3*-associated RP. Given that *NR2E3* likely slows degeneration, a booster may be necessary at minimum 6 months after initial treatment to maintain reduced degeneration. Future studies can evaluate the efficacy of a booster in a longitudinal study, and the efficacy of combination therapies. Further studies will examine the efficacy of *NR2E3* therapy in other non-*NR2E3*-associated forms of RP. This pharmacology study is translational to dosage selection, longitudinal effectiveness, and disease treatment stage for AAV5-hNR2E3 therapy in clinical trials currently underway for various forms of RP and Leber Congenital Amaurosis (ClinicalTrials.gov Identifier: NCT05203939).

DATA AVAILABILITY
All data used in this paper has been presented in the figures and supplementary files.

REFERENCES
1. Hamel C. Retinitis pigmentosa. Orphanet J Rare Dis. 2006;1:40.
2. al-Maghtheh M, Inglehearn CF, Keen TJ, Evans K, Moore AT, Jay M, et al. Identi-fication of a sixth locus for autosomal dominant retinitis pigmentosa on chro-mosome 19. Hum Mol Genet. 1994;3:351–4.
3. Andréasson S, Ponjavic V, Abrahamson M, Ehinger B, Wu W, Fujita R, et al. Phenotypes in three Swedish families with X-linked retinitis pigmentosa caused by different mutations in the RPGR gene. Am J Ophthalmol. 1997;124:95–102.

4. Blanton SH, Heckenlively JR, Cottingham AW, Friedman J, Sadler LA, Wagner M, et al. Linkage mapping of autosomal dominant retinitis pigmentosa (RP1) to the pericentric region of human chromosome 8. Genomics. 1991;11:857–69.

5. Ali MU, Rahman MSU, Cao J, Yuan PX. Genetic characterization and disease mechanism of retinitis pigmentosa; current scenario. 3 Biotech. 2017;7:251.

6. Ferrari S, Di Iorio E, Barbaro V, Ponzin D, Sorrentino FS, Parmeggiani F. Retinitis pigmentosa: genes and disease mechanisms. Curr Genomics. 2011;12:238–49.

7. Daiger SP, Sullivan LS, Bowne SJ. Genes and mutations causing retinitis pigmentosa. Clin Genet. 2013;84:132–41.

8. Bunker CH, Berson EL, Bromley WC, Hayes RP, Roderick TH. Prevalence of retinitis pigmentosa in Maine. Am J Ophthalmol. 1984;97:357–65.

9. Grøndahl J. Estimation of prognosis and prevalence of retinitis pigmentosa and Usher syndrome in Norway. Clin Genet. 1987;31:255–64.

10. Pierrottet CO, Zuntini M, Digiuni M, Bazzanella I, Ferri P, Paderni R, et al. Syndromic and non-syndromic forms of retinitis pigmentosa: a comprehensive Italian clinical and molecular study reveals new mutations. Genet Mol Res. 2014;13:8815–33.

11. Ahmed ZM, Riazuddin S, Riazuddin S, Wilcox ER. The molecular genetics of Usher syndrome. Clin Genet. 2003;63:431–44.

12. Boughman JA, Vernon M, Shaver KA. Usher syndrome: definition and estimate of prevalence from two high-risk populations. J Chronic Dis. 1983;36:595–603.

13. Beales PL, Warner AM, Hitman GA, Thakker R, Flinter FA. Bardet-Biedl syndrome: a molecular and phenotypic study of 18 families. J Med Genet. 1997;34:92–8.

14. Cox GF, Hansen RM, Quinn N, Fulton AB. Retinal function in carriers of Bardet-Biedl syndrome. Arch Ophthalmol. 2003;121:804–10.

15. Cross N, van Steen C, Zegaoui Y, Satherley A, Angelillo L. Retinitis pigmentosa: burden of disease and current unmet needs. Clin Ophthalmol. 2022;16:1993–2010.

16. Commissioner O of the. FDA. FDA. FDA approves novel gene therapy to treat patients with a rare form of inherited vision loss. 2020 [cited 2023 Sep 5]. Available from: https://www.fda.gov/news-events/press-announcements/fda-approves-novel-gene-therapy-treat-patients-rare-form-inherited-vision-loss.

17. Miraldi Utz V, Coussa RG, Antaki F, Traboulsi EI. Gene therapy for RPE65-related retinal disease. Ophthalmic Genet. 2018;39:671–7.

18. Kwak JJ, Kim HR, Byeon SH. Short-term outcomes of the first in vivo gene therapy for RPE65-mediated retinitis pigmentosa. Yonsei Med J. 2022;63:701–5.

19. Li S, Datta S, Brabbit E, Love Z, Woytowicz V, Flattery K, et al. Nr2e3 is a genetic modifier that rescues retinal degeneration and promotes homeostasis in multiple models of retinitis pigmentosa. Gene Ther. 2021;28:223–41.

20. Sohocki MM, Daiger SP, Bowne SJ, Rodriquez JA, Northrup H, Heckenlively JR, et al. Prevalence of mutations causing retinitis pigmentosa and other inherited retinopathies. Hum Mutat. 2001;17:42–51.

21. Houlston RS, Tomlinson IP. Modifier genes in humans: strategies for identification. Eur J Hum Genet. 1998;6:80–8.

22. Harper AR, Nayee S, Topol EJ. Protective alleles and modifier variants in human health and disease. Nat Rev Genet. 2015;16:689–701.

23. Chow CY, Kelsey KJP, Wolfner MF, Clark AG. Candidate genetic modifiers of retinitis pigmentosa identified by exploiting natural variation in Drosophila. Hum Mol Genet. 2016;25:651–9.

24. Haider NB, Ikeda A, Naggert JK, Nishina PM. Genetic modifiers of vision and hearing. Hum Mol Genet. 2002;11:1195–206.

25. Hsieh CS, Macatonia SE, O'Garra A, Murphy KM. T cell genetic background determines default T helper phenotype development in vitro. J Exp Med. 1995;181:713–21.

26. Kiesewetter S, Macek M, Davis C, Curristin SM, Chu CS, Graham C, et al. A mutation in CFTR produces different phenotypes depending on chromosomal background. Nat Genet. 1993;5:274–8.

27. Rose-Hellekant TA, Gilchrist K, Sandgren EP. Strain background alters mammary gland lesion phenotype in transforming growth factor-alpha transgenic mice. Am J Pathol. 2002;161:1439–47.

28. Calhoun JD, Hawkins NA, Zachwieja NJ, Kearney JA. Cacna1g is a genetic modifier of epilepsy in a mouse model of Dravet syndrome. Epilepsia. 2017;58:e111–5.

29. Eshraghi M, McFall E, Gibeault S, Kothary R. Effect of genetic background on the phenotype of the Smn2B/- mouse model of spinal muscular atrophy. Hum Mol Genet. 2016;25:4494–506.

30. Tanabe LM, Martin C, Dauer WT. Genetic background modulates the phenotype of a mouse model of DYT1 dystonia. PLoS ONE. 2012;7:e32245.

31. Ebermann I, Phillips JB, Liebau MC, Koenekoop RK, Schermer B, Lopez I, et al. PDZD7 is a modifier of retinal disease and a contributor to digenic Usher syndrome. J Clin Invest. 2010;120:1812–23.

32. Maddox DM, Ikeda S, Ikeda A, Zhang W, Krebs MP, Nishina PM, et al. An allele of microtubule-associated protein 1A (Mtap1a) reduces photoreceptor degeneration in Tulp1 and Tub mutant mice. Invest Ophthalmol Vis Sci. 2012;53:1663–9.

33. Fernandez-Funez P, Nino-Rosales ML, de Gouyon B, She WC, Luchak JM, Martinez P, et al. Identification of genes that modify ataxin-1-induced neurodegeneration. Nature. 2000;408:101–6.

34. Schorderet DF, Escher P. NR2E3 mutations in enhanced S-cone sensitivity syndrome (ESCS), Goldmann-Favre syndrome (GFS), clumped pigmentary retinal degeneration (CPRD), and retinitis pigmentosa (RP). Hum Mutat. 2009;30:1475–85.

35. Cruz NM, Yuan Y, Leehy BD, Baid R, Kompella U, DeAngelis MM, et al. Modifier genes as therapeutics: the nuclear hormone receptor Rev Erb alpha (Nr1d1) rescues Nr2e3 associated retinal disease. PLoS ONE. 2014;9:e87942.

36. Haider NB, Jacobson SG, Cideciyan AV, Swiderski R, Streb LM, Searby C, et al. Mutation of a nuclear receptor gene, NR2E3, causes enhanced S cone syndrome, a disorder of retinal cell fate. Nat Genet. 2000;24:127–31.

37. Sharon D, Sandberg MA, Caruso RC, Berson EL, Dryja TP. Shared mutations in NR2E3 in enhanced S-cone syndrome, Goldmann-Favre syndrome, and many cases of clumped pigmentary retinal degeneration. Arch Ophthalmol. 2003;121:1316–23.

38. Coppieters F, Leroy BP, Beysen D, Hellemans J, De Bosscher K, Haegeman G, et al. Recurrent mutation in the first zinc finger of the orphan nuclear receptor NR2E3 causes autosomal dominant retinitis pigmentosa. Am J Hum Genet. 2007;81:147–57.

39. Gire AI, Sullivan LS, Bowne SJ, Birch DG, Hughbanks-Wheaton D, Heckenlively JR, et al. The Gly56Arg mutation in NR2E3 accounts for 1-2% of autosomal dominant retinitis pigmentosa. Mol Vis. 2007;13:1970–5.

40. Webber AL, Hodor P, Thut CJ, Vogt TF, Zhang T, Holder DJ, et al. Dual role of Nr2e3 in photoreceptor development and maintenance. Exp Eye Res. 2008;87:35–48.

41. Cheng H, Aleman TS, Cideciyan AV, Khanna R, Jacobson SG, Swaroop A. In vivo function of the orphan nuclear receptor NR2E3 in establishing photoreceptor identity during mammalian retinal development. Hum Mol Genet. 2006;15:2588–602.

42. Sudharsan R, Beltran WA. Progress in gene therapy for rhodopsin autosomal dominant retinitis pigmentosa. Adv Exp Med Biol. 2019;1185:113–8.

43. Haeri M, Knox BE. Rhodopsin mutant P23H destabilizes rod photoreceptor disk membranes. PLoS ONE. 2012;7:e30101.

44. Humphries MM, Rancourt D, Farrar GJ, Kenna P, Hazel M, Bush RA, et al. Retinopathy induced in mice by targeted disruption of the rhodopsin gene. Nat Genet. 1997;15:216–9.

45. Sakami S, Maeda T, Bereta G, Okano K, Golczak M, Sumaroka A, et al. Probing mechanisms of photoreceptor degeneration in a new mouse model of the common form of autosomal dominant retinitis pigmentosa due to P23H opsin mutations. J Biol Chem. 2011;286:10551–67.

46. Noorwez SM, Sama RRK, Kaushal S. Calnexin improves the folding efficiency of mutant rhodopsin in the presence of pharmacological chaperone 11-cis-retinal. J Biol Chem. 2009;284:33333–42.

47. Noorwez SM, Kuksa V, Imanishi Y, Zhu L, Filipek S, Palczewski K, et al. Pharmacological chaperone-mediated in vivo folding and stabilization of the P23H-opsin mutant associated with autosomal dominant retinitis pigmentosa. J Biol Chem. 2003;278:14442–50.

48. Noorwez SM, Malhotra R, McDowell JH, Smith KA, Krebs MP, Kaushal S. Retinoids assist the cellular folding of the autosomal dominant retinitis pigmentosa opsin mutant P23H. J Biol Chem. 2004;279:16278–84.

49. Pasquale RL, Guo Y, Umino Y, Knox B, Solessio E. Temporal contrast sensitivity increases despite photoreceptor degeneration in a mouse model of retinitis pigmentosa. eNeuro. 2021;8:ENEURO.0020-21.2021.

50. Chiang WC, Kroeger H, Sakami S, Messah C, Yasumura D, Matthes MT, et al. Robust endoplasmic reticulum-associated degradation of rhodopsin precedes retinal degeneration. Mol Neurobiol. 2015;52:679–95.

51. Danciger M, Blaney J, Gao YQ, Zhao DY, Heckenlively JR, Jacobson SG, et al. Mutations in the PDE6B gene in autosomal recessive retinitis pigmentosa. Genomics. 1995;30:1–7.

52. Mitra RN, Zheng M, Weiss ER, Han Z. Genomic form of rhodopsin DNA nanoparticles rescued autosomal dominant Retinitis pigmentosa in the P23H knock-in mouse model. Biomaterials. 2018;157:26–39.

53. Mollema NJ, Yuan Y, Jelcick AS, Sachs AJ, von Alpen D, Schorderet D, et al. Nuclear receptor Rev-erb alpha (Nr1d1) functions in concert with Nr2e3 to regulate transcriptional networks in the retina. PLoS ONE. 2011;6:e17494.

54. Benchorin G, Calton MA, Beaulieu MO, Vollrath D. Assessment of murine retinal function by electroretinography. Bio-Protoc. 2017;7:e2218.

55. Haider NB, Zhang W, Hurd R, Ikeda A, Nystuen AM, Naggert JK, et al. Mapping of genetic modifiers of Nr2e3 rd7/rd7 that suppress retinal degeneration and restore blue cone cells to normal quantity. Mamm Genome Off J Int Mamm Genome Soc. 2008;19:145–54.

56. Olivares AM, Jelcick AS, Reinecke J, Leehy B, Haider A, Morrison MA, et al. Multimodal regulation orchestrates normal and complex disease states in the retina. Sci Rep. 2017;7:690.

57. Lotery AJ, Yang GS, Mullins RF, Russell SR, Schmidt M, Stone EM, et al. Adeno-associated virus type 5: transduction efficiency and cell-type specificity in the primate retina. Hum Gene Ther. 2003;14:1663–71.

58. Yang GS, Schmidt M, Yan Z, Lindbloom JD, Harding TC, Donahue BA, et al. Virus-mediated transduction of murine retina with adeno-associated virus: effects of viral capsid and genome size. J Virol. 2002;76:7651–60.

59. Pang JJ, Lauramore A, Deng WT, Li Q, Doyle TJ, Chiodo V, et al. Comparative analysis of in vivo and in vitro AAV vector transduction in the neonatal mouse retina: effects of serotype and site of administration. Vision Res. 2008;48:377–85.

60. Frederick A, Sullivan J, Liu L, Adamowicz M, Lukason M, Raymer J, et al. Engineered capsids for efficient gene delivery to the retina and cornea. Hum Gene Ther. 2020;31:756–74.

61. Kong F, Li W, Li X, Zheng Q, Dai X, Zhou X, et al. Self-complementary AAV5 vector facilitates quicker transgene expression in photoreceptor and retinal pigment epithelial cells of normal mouse. Exp Eye Res. 2010;90:546–54.

62. Petit L, Ma S, Cheng SY, Gao G, Punzo C. Rod outer segment development influences AAV-mediated photoreceptor transduction after subretinal injection. Hum Gene Ther. 2017;28:464–81.

63. Long BR, Sandza K, Holcomb J, Crockett L, Hayes GM, Arens J, et al. The impact of pre-existing immunity on the non-clinical pharmacodynamics of AAV5-based gene therapy. Mol Ther Methods Clin Dev. 2019;13:440–52.

64. Hetz C, Glimcher LH. Fine tuning of the unfolded protein response: assembling the IRE1α interactome. Mol Cell. 2009;35:551–61.

65. Alavi MV, Chiang WC, Kroeger H, Yasumura D, Matthes MT, Iwawaki T, et al. In vivo visualization of endoplasmic reticulum stress in the retina using the ERAI reporter mouse. Invest Ophthalmol Vis Sci. 2015;56:6961–70.

66. Chiang WC, Messah C, Lin JH. IRE1 directs proteasomal and lysosomal degradation of misfolded rhodopsin. Mol Biol Cell. 2012;23:758–70.

COMPETING INTERESTS
The authors declare no competing interests.

ETHICAL APPROVAL
This study was carried out in strict accordance with the recommendations in the Guide for the Care and Use of Laboratory Animals of the National Institute of Health, as well as the Association for Research in Vision and Ophthalmology (ARVO) Statement for the Use of Animals in Ophthalmic and Vision Research.

ADDITIONAL INFORMATION
Supplementary information The online version contains supplementary material available at https://doi.org/10.1038/s41434-024-00440-6.

Correspondence and requests for materials should be addressed to Neena B. Haider.

Reprints and permission information is available at http://www.nature.com/reprints

Publisher's note Springer Nature remains neutral with regard to jurisdictional claims in published maps and institutional affiliations.